

13. S. R. Jordan and C. O. Pabo, *ibid.* **242**, 893 (1988); A. K. Aggarwal *et al.*, *ibid.*, p. 899; Z. Otwinowski *et al.*, *Nature* **335**, 321 (1988).
14. D. Bohmann and R. Tjian, *Cell* **59**, 709 (1989).
15. S. Y. M. Lau *et al.*, *J. Biol. Chem.* **266**, 13253 (1984); R. S. Hodges *et al.*, *ibid.* **256**, 1214 (1981).
16. Y-H. Chen, J. T. Yang, K. H. Chau, *Biochemistry* **13**, 3350 (1974).
17. N. Greenfield and G. D. Fasman, *ibid.* **8**, 4108 (1969).
18. C. N. Pace, *Methods Enzymol.* **131**, 266 (1986); J. U. Bowie and R. T. Sauer, *Biochemistry* **28**, 7139 (1989).
19. T. D. Tullius, *Annu. Rev. Biophys. Biophys. Chem.* **18**, 213 (1989).
20. W. Sanger, in *Principles of Nucleic Acid Structure*, C. R. Cantor, Ed. (Springer-Verlag, New York, 1984), p. 371.
21. W. F. DeGrado, *Adv. Prot. Chem.* **39**, 51 (1988); E. T. Kaiser and F. J. Kézdy, *Science* **223**, 249 (1984); J. W. Taylor and E. T. Kaiser, *Pharmacol. Rev.* **38**, 291 (1986).
22. A. M. Labhardt *et al.*, *Biochemistry* **22**, 321 (1983).
23. A. M. Labhardt, *Proc. Natl. Acad. Sci. U.S.A.* **81**, 7674 (1984).
24. Amino acid sequences are tabulated in M. Nishizawa *et al.*, *ibid.* **86**, 7711 (1989). Abbreviations for the amino acid residues are: A, Ala; C, Cys; D, Asp; E, Glu; F, Phe; G, Gly; H, His; I, Ile; K, Lys; L, Leu; M, Met; N, Asn; P, Pro; Q, Gln; R, Arg; S, Ser; T, Thr; V, Val; W, Trp; and Y, Tyr.
25. S. Anott and D. W. L. Hukins, *Biochem. Biophys. Res. Commun.* **47**, 1504 (1972).
26. B. C. Finzel *et al.*, *J. Mol. Biol.* **186**, 627 (1985).
27. M. J. McGregor *et al.*, *ibid.* **198**, 295 (1987).
28. R. E. Brucoleri, J. Novotny, P. Keck, C. Cohen, *Biophys. J.* **49**, 79 (1986).
29. A. Maxam and W. Gilbert, *Methods Enzymol.* **65**, 497 (1980).
30. A. R. Oliphant, C. J. Brandl, K. Struhl, *Mol. Cell. Biol.* **9**, 2944 (1989).
31. We thank S. Jackson for peptide synthesis, J. Wendoloski and J. Krywko for expert assistance in model building, D. Janvic for amino acid analyses and oligonucleotide synthesis, C. Ampe and T. Steitz for their gift of GCN4, R. Steed for oligonucleotide purification, J. Lazaar for mass spectrometry, J. Blancy and W. Ripka for the use of a program to calculate DNA helices, and J. Novotny for sending coordinates of their model of an α -helical coiled coil. We also thank S. Brenner for helpful discussions and encouragement during the course of the work.

15 March 1990; accepted 20 June 1990.

Rapid, Sensitive Bioluminescent Reporter Technology for Naphthalene Exposure and Biodegradation

J. M. H. KING, P. M. DIGRAZIA, B. APPLGATE, R. BURLAGE,
J. SANSEVERINO, P. DUNBAR, F. LARIMER, G. S. SAYLER*

A bioluminescent reporter plasmid for naphthalene catabolism (pUTK21) was developed by transposon (Tn4431) insertion of the *lux* gene cassette from *Vibrio fischeri* into a naphthalene catabolic plasmid in *Pseudomonas fluorescens*. The insertion site of the *lux* transposon was the *nahG* gene encoding for salicylate hydroxylase. Luciferase-mediated light production from *P. fluorescens* strains harboring this plasmid was induced on exposure to naphthalene or the regulatory inducer metabolite, salicylate. In continuous culture, light induction was rapid (15 minutes) and was highly responsive to dynamic changes in naphthalene exposure. Strains harboring pUTK21 were responsive to aromatic hydrocarbon contamination in Manufactured Gas Plant soils and produced sufficient light to serve as biosensors of naphthalene exposure and reporters of naphthalene biodegradative activity. The robust and sensitive nature of the bioluminescent reporter technology suggests that new sensing methods can be developed for on-line process monitoring and control in complex environmental matrices.

BIOLUMINESCENCE IS A NATURAL phenomenon associated with several species, notably the firefly (*Photinus pyralis*) and the microorganisms *Photobacterium* and *Vibrio*. Expression and regulation of the bacterial luciferase (*lux*) genes has been studied in detail (1). The *lux* structural genes have been cloned and introduced into a variety of hosts (2). Recently, a light-emitting transcriptional fusion of the *lux* genes

from *Vibrio fischeri* and the upper pathway promoter from the catabolic plasmid NAH7 was developed as a direct measure of catabolic gene induction and expression (3). The use of bioluminescent light as a measure of catabolic activity offers attractive applications in environmental simulations and potential field analysis for on-line analysis of microbial biodegradative activity. In comparison to conventional activity assays, bioluminescent reporter systems are noninvasive, nondestructive, rapid, and population-specific.

We describe here the construction and characterization of a bioluminescent reporter plasmid for naphthalene degradation. The application of this bioluminescent reporter system in conjunction with remote sensing

technology for monitoring in situ biodegradative activity in environmental simulations was also demonstrated. A photomultiplier detection system was developed to quantify bioluminescence (3, 4). This type of monitoring system has distinct advantages over previous methods, such as autoradiography and scintillation counting, in that it is rapid and sensitive and it permits on-line and in situ determinations of bioluminescence.

The bioluminescent reporter plasmid (pUTK21) for naphthalene catabolism was constructed by transposon mutagenesis of a *Pseudomonas fluorescens* strain 5R with the use of the *lux* transposon Tn4431 carried on the suicide vector plasmid pUCD623 (Fig. 1A). Strain 5R is an environmental isolate from a Manufactured Gas Plant (MGP) soil. The naphthalene catabolic genes are encoded on a plasmid, pKA1, that shows homology to the archetypal naphthalene catabolic plasmid, NAH7 (5). In NAH7 the catabolic genes are organized into two operons, an upper pathway operon encoding for the conversion of naphthalene to salicylate and a lower pathway operon encoding for the oxidation of salicylate to acetaldehyde and pyruvate. Induction of the two operons is controlled at the transcriptional level not by naphthalene but by its metabolite, salicylate, and by the product of the regulatory gene, *nahR* (6).

We selected the bioluminescent construct 5RL, containing plasmid pUTK21, on the basis of its ability to produce strong inducible light when exposed to naphthalene vapor or when grown in the presence of salicylate. Biochemical and genetic mapping evidence was used to determine the probable insertion site of the *lux* transposon. Strain 5RL did not mineralize naphthalene completely and it accumulated salicylate (7), indicating that the insertion is in the lower-pathway operon. By restriction mapping and preliminary DNA blot hybridization analysis, we were able to localize the *lux* transposon to a 1.6-kb Pst I fragment adjacent to the *nahH* gene (8). On the basis of the biochemical data, and by assuming an NAH7-like organization of the lower pathway operon, we propose that the *lux* transposon inserted in the *nahG* (salicylate hydroxylase) gene (Fig. 1B).

The bioluminescent catabolic reporter plasmid pUTK21 was transferred by conjugation to another environmental *P. fluorescens* strain, strain HK9 (9). This strain was isolated from an MGP soil and was able to degrade salicylate but not naphthalene (Nah⁻Sal⁺ phenotype). The recipient strain HK44 containing pUTK21 has a Nah⁺Sal⁺ phenotype and exhibited the same light-producing characteristics as strain 5RL.

We evaluated the dynamic response of the

J. M. H. King, P. M. DiGrazia, B. Applegate, R. Burlage, J. Sanseverino, P. Dunbar, G. S. Sayler, Center for Environmental Biotechnology, University of Tennessee, 10515 Research Drive, Suite 200, Knoxville, TN 37932.

F. Larimer, Biology Division, Oak Ridge National Laboratory, Oak Ridge, TN 37831.

*To whom correspondence should be addressed.

bioluminescent reporter strain HK44 to periodic controlled variations in naphthalene exposure in a continuous culture system. The experimental system consisted of a 1-liter chemostat reactor with on-line off-gas sampling for time series determination of the naphthalene off-gas concentration (10). Bioluminescence was measured with the photomultiplier detection system (4).

We started the chemostat experiments (11) by establishing steady state with the nonnaphthalene feed source. Naphthalene feed to the chemostat was then initiated. After a 15-min lag period, we observed a linear increase in light production at a rate of $0.72 \mu\text{A hour}^{-1}$, followed by a reduction in light output to a steady-state level of $1.1 \mu\text{A}$ (Fig. 2). Although the liquid naphthalene concentration in the reactor, calculated from Henry's law (12), increased linearly and leveled off to a steady-state concentration of $200 \mu\text{g liter}^{-1}$ after ~ 2 hours, the rate of naphthalene degradation remained constant (Fig. 2).

Square-wave perturbations in naphthalene feed concentration (or naphthalene feed rate, because the total flow rate is held constant) were used to determine the dynamic light response of strain HK44. In the 4-hour cycle, light production increased linearly at a rate of $0.39 \mu\text{A hour}^{-1}$ during the 2-hour naphthalene exposure period, followed by a near linear reduction in light output during the 2-hour period with no naphthalene feed (Fig. 3). In each cycle, the liquid naphthalene concentration in the chemostat increased to a steady-state concentration between 0.4 and $0.5 \text{ mg liter}^{-1}$. When

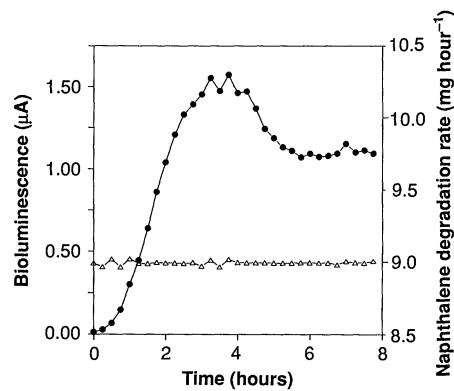


Fig. 2. Induction of bioluminescence of strain HK44 (pUTK21) in continuous culture: (●) bioluminescence and (Δ) naphthalene degradation rate. Data represent single time point determinations, and the results are representative of three independent experiments.

the naphthalene feed was stopped, the reactor naphthalene concentration exponentially decreased to $0.1 \text{ mg liter}^{-1}$. A reduction in the rate of increase in light production from 0.39 to $0.26 \mu\text{A hour}^{-1}$ was observed when the feed concentration to the system was reduced from 30 to 18 mg liter^{-1} during the final cycle (Fig. 3). These data suggest that bioluminescence may be proportional to the naphthalene degradation rate.

We performed four additional square-wave perturbation experiments with cycle lengths of 0.5 , 2 , 8 , and 16 hours (Fig. 4). The responses in bioluminescence that we observed in these experiments were consistent with the observed responses in the steady-state (Fig. 2) and 4-hour perturbation (Fig. 3) experiments. A 15-min lag in

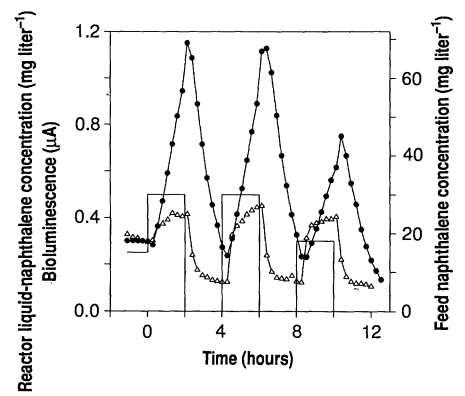


Fig. 3. Dynamic response to 4-hour square-wave perturbations in naphthalene: (●) bioluminescence; (—) naphthalene feed concentration; and (Δ) reactor liquid-naphthalene concentration. The results were obtained from a single experiment and are characteristic of similar independent experiments reported.

bioluminescent response to changes in naphthalene exposure was observed in all cases. This lag forced the light response out of phase with the feed cycle at the short cycle times (Fig. 4, A and B). Bioluminescence peaked near an exposure time of 4 hours (Figs. 2 and 4, C and D) and began to decline to a steady-state level if naphthalene exposure continued (Figs. 2 and 4D). When the naphthalene exposure period was longer

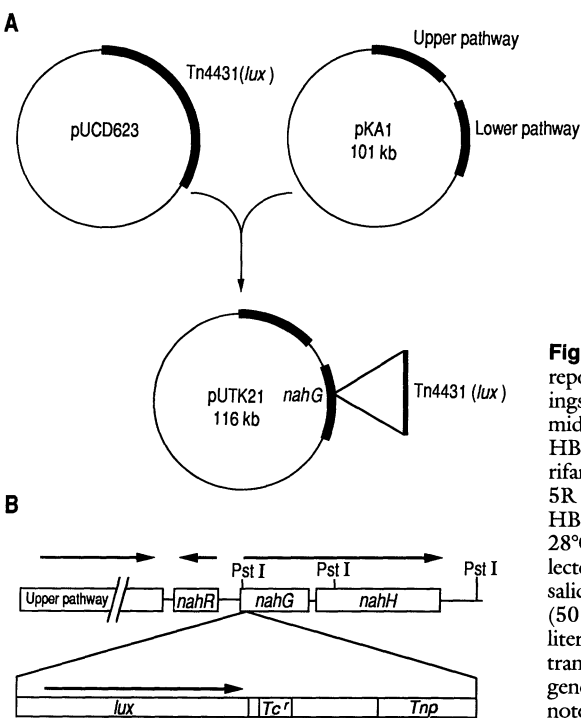


Fig. 1. Construction of bioluminescent reporter plasmid pUTK21. (A) Filter matings were performed with a 1:10 ratio of mid-log phase cultures of *Escherichia coli* HB101 (pUCD623) and a spontaneous rifampicin-resistant mutant of *P. fluorescens* 5R (pKA1). After incubating strain HB101 and strain 5R for 24 hours at 28°C , bioluminescent constructs were selected on yeast extract, peptone, succinate, salicylate agar (3) containing rifampicin (50 mg liter^{-1}), and tetracycline (14 mg liter^{-1}). (B) Proposed location of the *lux* transposon in pUTK21. *Tnp* denotes genes required for transposition. *Tc^r* denotes tetracycline resistance gene.

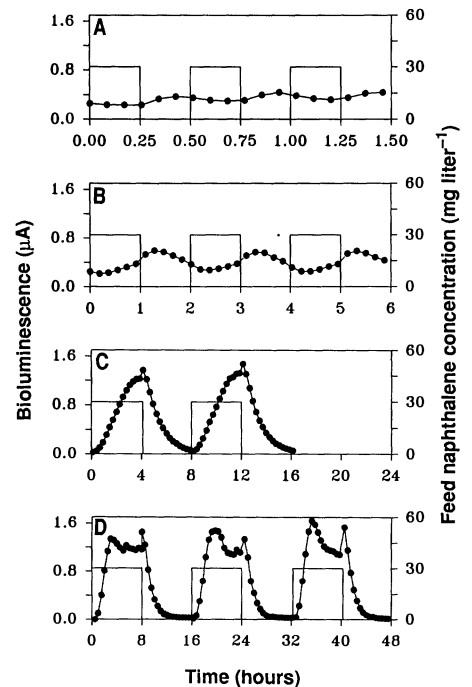


Fig. 4. Bioluminescence response to square-wave perturbations in naphthalene feed concentration (rate): (A) 0.5-hour cycle; (B) 2-hour cycle; (C) 8-hour cycle; and (D) 16-hour cycle. (●) Bioluminescence and (—) naphthalene feed concentration. Perturbation cycles were repeated at each frequency to demonstrate the reproducibility of the bioluminescent response. The results are representative of two independent experiments.

than 2 hours and bioluminescence was high, a rapid, transient increase in bioluminescence occurred when naphthalene was eliminated from the feed (Figs. 3 and 4, C and D). In contrast, the naphthalene degradation rate was constant and nearly equal to the feed rate during the exposure periods and was negligible when no naphthalene was being fed to the system.

These experiments demonstrated that light production from strain HK44 was related to naphthalene exposure and degradation rate. The complex light output behavior was probably not a gene regulation effect, since complex changes in naphthalene degradation rate were not observed, and both naphthalene degradation and light output of strain HK44 are under the same regulation. A more likely hypothesis is that the light response was affected by dynamic interactions of the components of the light-producing and naphthalene catabolic pathways, that is, O₂, adenosine triphosphate (ATP), aldehyde, luciferase, and so forth. For example, both pathways compete for O₂ from a common pool within the cell. Further experimentation is necessary to elucidate mechanisms that account for this complex behavior.

The application of the bioluminescent reporter technology for in situ analysis was demonstrated in a series of soil slurry experiments in which contaminated and uncontaminated soils were used (Fig. 5). We prepared slurries by adding a suspension of uninduced HK44 cells to the soil, and we monitored bioluminescence by placing the liquid light pipe detection probe into the slurry matrix. Bioluminescence, indicative of naphthalene exposure and degradative activity, was observed in an MGP soil (13) naturally contaminated with polycyclic aromatic hydrocarbons (PAH), and in the control soil (13) to which naphthalene was added (Fig. 5). No bioluminescent activity was detected in the uncontaminated control soil. In contrast to the 15-min lag in the chemostat studies, a 1-hour lag period occurred before bioluminescence was detected in the soil slurry experiments. This extended lag period can probably be attributed to quenching of the light and interference in the detection system by the soil matrix. A transient peak in bioluminescence of 0.75 nA occurred in the MGP soil slurry at 6 hours followed by a constant light output of 0.31 nA. In the control soil with added naphthalene, there was no transient peak and bioluminescence leveled off after 6 hours at 0.1 nA. Because of differences in the soil slurry matrices, the results in Fig. 5 give only a qualitative indication of biodegradative activity. Additional experiments would be required to correlate biolumines-

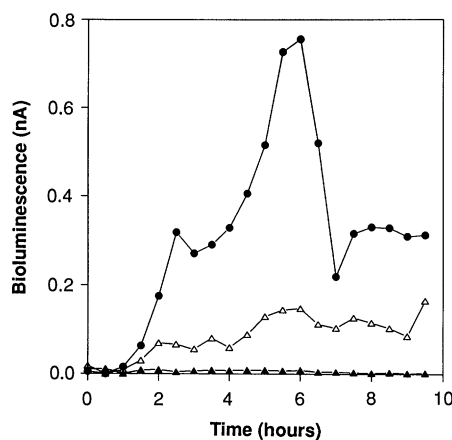


Fig. 5. Detection of bioluminescence in soil slurries containing strain HK44. The test system consisted of 10 g of soil and 10 ml of uninduced HK44 cells (10^9 cells per milliliter) in phosphate-buffered saline. The slurry was stirred to provide aeration, and we monitored the bioluminescence by placing the liquid light pipe into the slurry. (▲) Control soil; (△) control soil with 10 mg of naphthalene added; (●) MGP soil. The results are representative of two independent experiments.

cence levels in situ with actual biodegradative activity levels. The response observed in the MGP soil slurry illustrates the use of bioluminescence as a tool for determining the bioavailability of contaminants in environmental matrices such as soil or ground water.

Predictions of the environmental fate of pollutants and of controlled interventions in bioremediation of contaminated environments require quantitative knowledge of specific microbial populations and the corresponding biodegradative activity under in situ conditions. Recently, a variety of molecular techniques, such as nucleic acid extraction, hybridization, and analysis (14), have provided information on the presence and quantitative abundance of specific populations, catabolic genotypes, and genes, and on their maintenance in complex environmental matrices. These techniques help to define the structure and genetic potential of biodegradative communities but provide little or no information relating to the expression of specific genes or the activity of the organisms.

The results of this investigation demonstrate that *lux* transcriptional fusions with catabolic genes offer a useful molecular tool for direct analysis of biodegradative microbial activity in complex environmental matrices. This bioluminescent reporter technology can be used in simulations to optimize environmental regimes leading to sustained and predictable microbial biodegradation. It is anticipated that additional bioluminescent reporter plasmids or bacterial strains will be developed for other chemical agents. With

the development of appropriate cell immobilization techniques and fiber optic methods for remote light sensing it is expected that practical applications for bioluminescent reporters will be forthcoming as part of an on-line monitoring or process control technology. These applications will be particularly valuable in mixed culture biological processes, such as waste treatment, and in environmental systems such as ground water where bioluminescent reporters can act as specific sensors or sentinels of chemical agents. Of equal importance is the ability of this technology to rapidly measure and control the response of biosynthetic or biodegradative metabolic pathways to specific engineering practices or reactor configurations and operational regimes for mixed- or pure-culture systems.

REFERENCES AND NOTES

1. E. A. Meighan, *Annu. Rev. Microbiol.* **42**, 151 (1988).
2. J. J. Shaw, L. G. Settles, C. I. Kado, *Mol. Plant-Microbe Interact.* **1**, 39 (1987).
3. R. S. Burlage, G. S. Saylor, F. Larimer, *J. Bacteriol.*, in press.
4. Bioluminescence was detected with the use of an Oriel digital display (model 7070) with a photomultiplier tube (model 77340) connected to a flexible liquid light pipe and collimating beam probe. Sampling was controlled by an IBM PS/2 personal computer. Light detection is measured in amperes from a photoelectric-induced effect.
5. J. M. H. King, B. Applegate, G. S. Saylor, unpublished results.
6. K.-M. Yen and C. M. Serdar, *CRC Crit. Rev. Microbiol.* **15**, 247 (1988).
7. Naphthalene mineralization assays were performed in basal salts medium as described in (3). The cell concentration was 10^7 ml⁻¹, and naphthalene (100 mg liter⁻¹) was added as the sole carbon source together with 2×10^6 dpm of [¹⁴C]naphthalene. Samples were incubated for 48 hours at 25°C. Aqueous phase metabolites were analyzed by high-pressure liquid chromatography in conjunction with proportional counting of radiolabel fractions. Metabolites (200- μ l sample volume) were separated on a Supelcosil LC-18 column (flow rate, 2 ml min⁻¹) by elution for 5 min with water (pH 2.5) followed by a linear gradient to 60% acetonitrile: 40% water (5% min⁻¹). Detection was by a photodiode array detector at a wavelength of 255 nm. Eluant from the photodiode array detector was mixed on-line with scintillation cocktail (6 ml min⁻¹) and passed through a Flo-One Beta Radioactive Flow Detector Model IC/CR. [¹⁴C]Salicylate was identified as the sole metabolite by measurement of its retention time against known standards and by ultraviolet spectral analysis.
8. Plasmid DNA was isolated as described [D. G. Anderson and L. L. McKay, *Appl. Environ. Microbiol.* **46**, 549 (1983)]. Restriction endonuclease digestion and DNA blot analysis were accomplished as described [T. Maniatis, E. F. Fritsch, J. Sambrook, *Molecular Cloning: A Laboratory Manual* (Cold Spring Harbor Laboratory, Cold Spring Harbor, NY, 1982)]. Location of the *nahH* gene was determined with a clone of *xylE* (obtained from S. Cuskey) that is homologous to *nahH*. Hybridization conditions were as described [G. S. Saylor et al., *Appl. Environ. Microbiol.* **49**, 1295 (1985)].
9. Filter matings were performed with a 1:10 ratio of donor (5RL) to recipient (HK9) cells. After incubating strain 5RL and strain HK9 for 24 hours at 25°C, transconjugants were selected on *Pseudomonas* isolation agar (Difco) containing tetracycline (14 mg liter⁻¹). Strain 5RL cannot grow on *Pseudomonas* isolation agar.

10. P. M. DiGrazia *et al.*, unpublished results.
11. The chemostat operating conditions were as follows: temperature, 25°C; dilution rate, 0.4 hour⁻¹; mean cell residence time, 2.5 hours. Feed consisted of a minimal salts medium (3) containing sodium succinate (100 mg liter⁻¹), yeast extract (100 mg liter⁻¹), and tetracycline (14 mg liter⁻¹); naphthalene was added to one of the two feed supplies at 30 mg liter⁻¹.
12. K. Truong and J. W. Blackburn, *Environ. Prog.* **3**, 143 (1984).
13. The MGP soil was obtained from a site in the northeastern United States. The total PAH concentration was 3227 mg kg⁻¹, of which 1240 mg kg⁻¹ was naphthalene. An uncontaminated Etowah soil obtained from East Tennessee was used as the control soil.
14. A. V. Ogram, G. S. Saylor, T. Barkay, *J. Microbiol. Methods* **7**, 57 (1987); G. S. Saylor, J. Fleming, B. Applegate, C. Werner, K. Nikbakht, in *Recent Advances in Microbial Ecology*, T. Hattori, Y. Ishida, Y. Maruyama, R. Y. Morita, A. Uchida, Eds. (Japan Scientific Societies Press, Tokyo, 1989), pp. 658–662.
15. Supported by the U.S. Geological Survey, Office of Water Research grant 14-08-0001-G1482, U.S. Air Force contract F49620-89-C-0023, Gas Research Institute contract 5087-253-1490, Electric Power Research Institute contract RP-3015-1, the University of Tennessee, Waste Management Research and Education Institute, and IT Corporation.

30 March 1990; accepted 8 June 1990

Antibody-Catalyzed Porphyrin Metallation

ANDREA G. COCHRAN AND PETER G. SCHULTZ*

An antibody elicited to a distorted *N*-methyl porphyrin catalyzed metal ion chelation by the planar porphyrin. At fixed Zn²⁺ and Cu²⁺ concentrations, the antibody-catalyzed reaction showed saturation kinetics with respect to the substrate mesoporphyrin IX (2) and was inhibited by the hapten, *N*-methylmesoporphyrin IX (1). The turnover number of 80 hour⁻¹ for antibody-catalyzed metallation of 2 with Zn²⁺ compares with an estimated value of 800 hour⁻¹ for ferrochelatase. The antibody also catalyzed the insertion of Co²⁺ and Mn²⁺ into 2, but it did not catalyze the metallation of protoporphyrin IX (3) or deuteroporphyrin IX (4). The antibody has high affinity for several metalloporphyrins, suggesting an approach to developing antibody-heme catalysts for redox or electron transfer reactions.

THE IMMUNE SYSTEM PRODUCES A repertoire of 10¹⁰ to 10¹² antibody molecules (1) that can recognize and bind a huge array of naturally occurring and synthetic molecules. Recently, the tremendous diversity and specificity of the immune response have been merged with our understanding of chemical processes to produce catalytic antibodies. Since the first reports of antibody catalysis (2), a wide variety of transformations have been examined (3). In addition, several general strategies have been developed for the rational design of catalytic antibodies. We report the generation of antibodies to a hapten that mimics a strained conformation of substrate. Antibodies specific for a distorted *N*-methyl porphyrin catalyze metal ion chelation by the corresponding planar, non-methylated porphyrin. This system expands the catalytic antibody repertoire to include ligand substitution reactions.

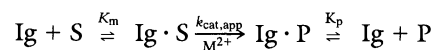
Ferrochelatase, the terminal enzyme in the heme biosynthetic pathway, catalyzes the insertion of Fe²⁺ into protoporphyrin IX (3) (4). *N*-methyl-protoporphyrin IX is a potent inhibitor of ferrochelatase with an inhibition constant (*K_i*) of 7 nM (5). The

distortion of the porphyrin macrocycle resulting from *N*-alkylation is thought to approximate the transition state of the enzymatic reaction (4, 6). Such bending would increase exposure of the pyrrole nitrogen lone pairs to solvent and thus facilitate metal ion complexation. Indeed, kinetic studies have shown that *N*-alkylporphyrins chelate metal ions 10³- to 10⁵-fold faster than their non-alkylated cognates (4). We reasoned that if *N*-methylporphyrins are in fact transition state analogs for porphyrin metallation, antibodies elicited to such compounds should catalyze metal ion incorporation by distortion of the corresponding substrate.

We prepared antibodies specific for *N*-methylmesoporphyrin IX (1) (isomer mixture, Porphyrin Products, Inc., Logan, Utah) (Fig. 1). We chose 2 as substrate rather than 3 because of the relative photosensitivity of the latter (7) and the greater tendency of 3 to aggregate in aqueous solution (8). In addition, several convenient ferrochelatase assays have been described that use mesoporphyrin as substrate (9–11). Three hybridoma lines were identified that produced antibodies specific for 1 (12). Two of the three purified antibodies catalyzed Zn(II) and Cu(II) mesoporphyrin formation. The faster of these, 7G12-A10-G1-A12, was characterized further (13).

The antibody-catalyzed reaction could be

described by the following scheme:



where S is porphyrin substrate, P is metalloporphyrin product, M²⁺ is metal, I_g is antibody, *K_m* is the Michaelis constant, *K_p* is the product inhibition constant, and *k_{cat,app}* is the *k_{cat}* (catalytic constant) observed with a particular fixed concentration of metal. Significant product inhibition by Zn(II) mesoporphyrin and the relative inaccuracy of the assay at small percentages of substrate conversion did not allow the determination of initial rates for this reaction. The data were therefore fit to the integrated form of Eq. 1 (14):

$$\frac{d[P]}{dt} = \frac{V_{max,app}[S]}{K_m(1 + [P]/K_p) + [S]} \quad (1)$$

Typical plots for different porphyrin concentrations at 1 mM Zn²⁺ are shown in Fig. 2 [*K_m* = 49 μM, *K_p* = 2.9 μM, and *V_{max,app}* (maximum apparent velocity) = 24 μM hour⁻¹]. The pseudo first-order rate constant for uncatalyzed metallation at the same Zn²⁺ concentration is 0.031 hour⁻¹. Chelation of Co²⁺ and Mn²⁺ was also catalyzed, but because of the much greater product inhibition and substantially slower reaction rates, no further kinetic characterization was attempted. Incorporation of Ni²⁺ was not catalyzed.

Copper(II) mesoporphyrin was not observed to inhibit antibody catalysis up to concentrations of at least 15 μM, allowing the determination of initial rates for production of this metalloporphyrin. A Lineweaver-Burk plot for antibody-catalyzed Cu²⁺ incorporation (1 mM Cu²⁺) gives a *K_m* for 2 of 50 μM, nearly identical to the value obtained with Zn²⁺, and a *V_{max,app}* of 2.6 μM hour⁻¹ (Fig. 3). The pseudo first-

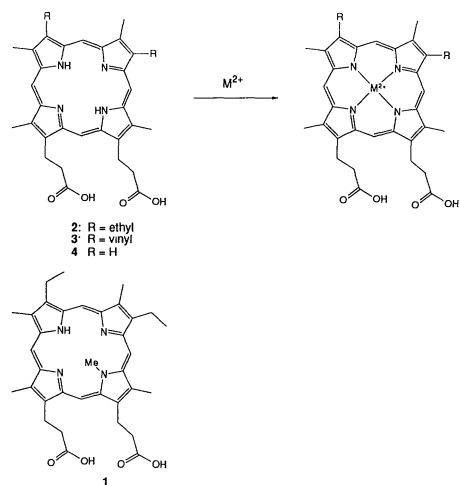


Fig. 1. Hapten and reaction scheme for metalloporphyrin formation.

Department of Chemistry, University of California, Berkeley, CA 94720.

*To whom correspondence should be addressed.